ACS Catalysis

Research Article

pubs.acs.org/acscatalysis

Operando Transmission Electron Microscopy: A Technique for Detection of Catalysis Using Electron Energy-Loss Spectroscopy in the Transmission Electron Microscope

Santhosh Chenna and Peter A. Crozier*

School for Engineering of Matter, Transport and Energy, Arizona State University, Tempe, Arizona 85287-6106, United States

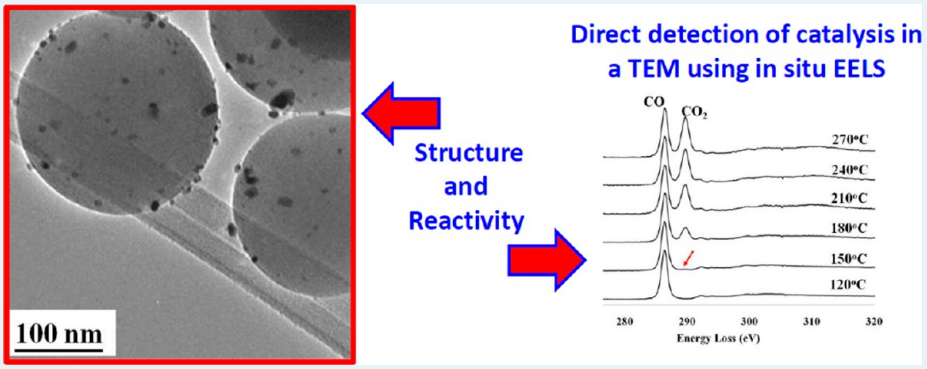

ABSTRACT: Operando studies have a significant impact in the field of heterogeneous catalysis for understanding the functionality of catalytic materials. Using operando techniques, dynamic structural changes of working catalysts can be obtained while measuring the catalytic performance at the same time. We have developed an "operando TEM" technique that combines the nanostructural characterization of the catalyst during the reaction with the simultaneous measurement of the catalyst activity using spectroscopy. Electron energy-loss spectroscopy (EELS) was employed to detect and quantify catalytic products directly inside the environmental cell of the transmission electron microscope. In this paper, a detailed discussion on some of the challenges associated with developing operando TEM has been presented along with the initial results demonstrating the feasibility of this technique.

KEYWORDS: *In-situ TEM, operando, ruthenium, EELS, heterogeneous catalysis*

1. INTRODUCTION

Catalysis plays an important role in the world economy. The global catalyst market estimates the global demand on catalysts was valued at US$29.5 billion in 2010 and will witness robust growth over the next few years.[1] There is always a constant push for developing novel catalytic materials or improving existing catalysts. Understanding structure−reactivity relations for catalysts is essential in developing a complete fundamental understanding of the functionality of catalytic materials. Catalysts can undergo several changes during a reaction; hence post-mortem studies after the reaction may not accurately represent the exact state of the catalyst during a reaction. The structure of a catalyst depends on several factors, such as temperature, pressure, reactant gases, product gases, and concentration of different gas species on the surface of the catalyst. Thus, to obtain information on the active state of a catalyst, it is important to apply in situ techniques that allow catalyst structure to be determined while catalytic reactions are taking place, that is, under the working conditions.

In situ environmental transmission electron microscopy (ETEM) is a powerful tool to study dynamic gas−solid interactions under reacting gas conditions at elevated temperatures and is ideal for studying high surface area materials that are often used as catalysts.[2−5] The ability to study catalytic materials at elevated temperatures in the presence of reactive gases can provide fundamental insights into the catalyst synthesis and its dynamic evolution during a catalytic reaction.[6−13] For example, by correlating catalytic reactor data with suitably designed ETEM observations, it is possible to map the structure−reactivity relations in catalysts.[14] However in this case, the catalytic measurements were performed in an ex situ reactor, and the nanostructural information is obtained from in situ ETEM studies. Ideally the conditions inside the ETEM should be identical to those in the flow reactor. In practice this is almost impossible to achieve because of the fundamental differences in reactor design. However, for suitable chosen systems where the reaction is not strongly dependent on pressure between 0.001 and 1 atm, identical conditions may not be strictly required and significant insights into the structure−reactivity relations can be determined.

Special Issue: Operando and In Situ Studies of Catalysis

Received: July 20, 2012
Revised: September 23, 2012
Published: October 3, 2012

   dx.doi.org/10.1021/cs3004853 | *ACS Catal.* 2012, 2, 2395−2402

It would be highly desirable to measure the activity and selectivity of the catalyst simultaneously with the structure so that the complete structure and reactivity could be directly correlated. This approach gives rise to the so-called operando methods first pioneered for Raman spectroscopy.[15] Until recently, true operando microscopy characterization was demonstrated for applications such as catalytic growth of polymers, nanotubes, and nanowires where the catalytic products were solids which can be directly imaged.[16−19] For example with nanotubes/wires, the kinetics of the growth process relates directly to the catalyst activity, and the type of wire growing relates directly to the catalyst selectivity. It was interesting to note that many of the initial attempts to observe catalytic materials growth failed often because of poisoning or passivation layers on the surface of the catalyst upon introduction to the TEM (e.g., Oleshko et al., 2002).[16] In each of these applications, the researchers had to determine suitable in situ processing procedures to activate the catalyst in the ETEM and observe product formation. These procedures vary from instrument to instrument and depend on the partial pressure and composition of the residual background gases in the vacuum system and the sensitivity of the catalyst to poisons.

There is no reason to suppose that catalysts used for gas (or liquid) phase reactions may not also be subject to the same deactivation processes when introduced into the ETEM. The degree to which this should be of concern will of course depend on the choice of catalytic material and the reaction under study. However, to be certain that the structure being observed in the ETEM is actually the active form of the catalyst it is necessary to prove that catalysis is actually occurring in the microscope. For gas phase reactions, the reactant and product gases are not directly visible with microscopy imaging and diffraction techniques and so suitable spectroscopic methods must be developed to detect the product gas molecules. However, the quantity of product synthesized by a typical TEM sample is too small to be measured by even the most sensitive mass spectrometers. Moreover, the surface area associated with the inside of the reaction chamber of the ETEM will easily be much larger than the volume of catalyst in a typical TEM sample.

While these problems are challenging they are not insurmountable and here we demonstrate that an "operando TEM" technique can be developed that combines measurement of the catalyst activity using spectroscopy with simultaneous nanostructural characterization of the catalyst material during the reaction. In our current set of experiments we employ electron energy-loss spectroscopy (EELS) to detect catalysis taking place inside the ETEM. Recently we demonstrated that electron energy loss spectroscopy in the TEM can be used to quantify the gas composition inside the reaction cell.[20] Here we extend this approach to demonstrate that catalytic products can be detected and quantified inside the microscope reaction cell while simultaneously determining the nanoscale structure of the catalyst. One advantage of using EELS is that the composition of the volume of gas adjacent to the TEM sample is directly measured. EELS is available on many microscopes, and this approach can be applied to ETEM based on differentially pumped cells, windowed cells, or cells fitted with injection needles.

This paper describes some of the challenges and opportunities for developing an operando TEM methodology and will demonstrate the direct detection of gas-phase catalysis in the environmental cell in the TEM. For proof of concept, two catalytic reactions were considered in this study: CO oxidation and CO_2 methanation. Ru is an efficient catalyst for both of these reactions,[21−24] and Ru supported on SiO_2 spheres was used as a model catalyst for both the reactions. In situ catalytic activity measurements were performed with EELS and confirmed that catalysis could be detected inside the TEM using EELS. Conventional catalytic reactions were also performed for comparison with the operando TEM experiments.

2. CONVENTIONAL CATALYTIC REACTOR VERSUS ETEM REACTOR

Before describing the results it is important to consider the differences in the conventional catalytic reactor and the environmental TEM (ETEM) reactor. Conventional catalytic activity measurements were performed in an external quartz tube flow reactor. An *In-Situ* Research Instruments (ISRI) RIG-150 reactor was used for measuring catalytic conversions, and a schematic of the reactor tube is shown in Figure 1. In the RIG-150 reactor, gas flows from the top of the reactor tube along the catalyst bed, and the product gas exiting the reactor is analyzed with gas chromatography. The flow rate and the composition of the gas is controlled by mass flow controllers. Catalyst powder is packed between glass wool which is then inserted into the quartz tube. For the flow rates and experiments involved here, most of the gas comes into contact with the catalysts, and the conversions can approach 100%.

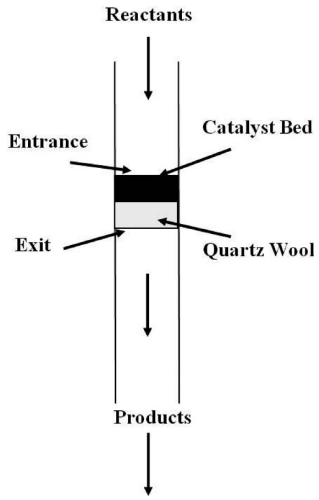

Figure 1. Schematic representation of ISRI RIG-150 reactor bed.

Operando TEM experiments were performed in an FEI Tecnai F20 field-emission environmental transmission electron microscope (ETEM) operating at 200 kV with a point resolution of 0.24 nm and an information limit of 0.13 nm. The instrument was equipped with a Gatan imaging filter allowing in situ electron energy-loss spectroscopy to be performed. Figure 2 shows a schematic of the environmental cell in a Tecnai F20 environmental TEM. The gas reaction cell or environmental cell (essentially a flow microreactor) of this instrument allows atomic-level observations of gas−solid interactions at pressures up to a few Torr and temperatures up to 800 °C. A Gatan Inconel heating holder was used for the ETEM reactions. This microscope is equipped with a differential pumping system to maintain high gas pressures near the sample region of the microscope and at the same time maintains low pressure in the column and preserves ultrahigh

dx.doi.org/10.1021/cs3004853 | ACS Catal. 2012, 2, 2395−2402

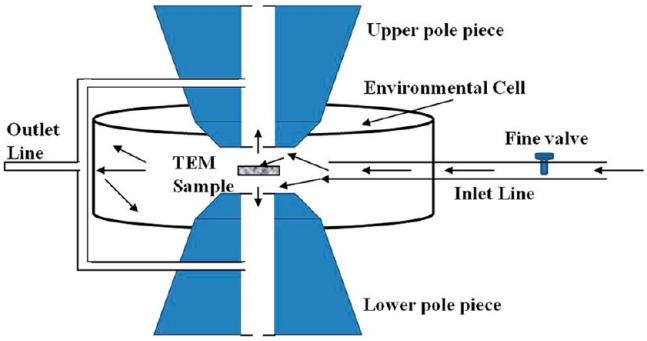

Figure 2. Schematic representation of ETEM reactor.

vacuum conditions at the electron source. Gases for the reaction are premixed in a tank in the desired ratio and introduced into the environmental cell through a leak valve. Gas eventually diffuses through the differential pumping apertures (of 100 μm in size) and is pumped out of the system. The ETEM reactor does not have a plug-flow geometry and is essentially a large bypass reactor. We have not done a detailed study of the gas flow through the cell although preliminary testing suggests that it takes a few minutes to completely refresh the gas within the cell. The volume of the cell in the Tecnai F20 is approximately 1000 cm^3, which is many orders of magnitude larger than the volume of catalyst in a typical TEM sample. In this case, gas can flow through the ETEM reactor without contacting the catalysts. Consequently, the catalytic conversions are very small giving a correspondingly low concentration of product gases.

The operating pressure and temperature profiles are different between the RIG-150 reactor and the ETEM reactor. The RIG-150 reactor works at 1 atm with reactant gas partial pressures typically ranging from 50 to 200 Torr (the balance is He carrier gas). The ETEM reactor experiments are typically performed at reactant gas pressures of about 1 Torr, and no carrier gas is used. In the RIG-150 reactor, almost all the length of the reactor tube is heated. The gas entering through the top of the reactor tube will be at the reaction temperature by the time it contacts the catalyst surface. In the ETEM reactor, the furnace occupies a very small volume of the reactor, and the gas admitted into the cell is at room temperature and will reach the reaction temperature only when it is in contact with the sample surface.

One of the challenges in developing an operando TEM technique is the very low conversions that typically take place in the ETEM reactor. The challenge here is to prepare a TEM sample with a large amount of catalyst, so that sufficiently high catalytic conversions can take place giving product gases that can be detectable by EELS.

3. SAMPLE PREPARATION FOR OPERANDO TEM

Ru nanoparticles supported on SiO_2 spheres were used as a model catalyst. A 2.5 wt % Ru/SiO_2 catalyst was prepared by impregnating SiO_2 spheres with ruthenium chloride hydrate ($RuCl_3{\cdot}xH_2O$) solution using an incipient wetness technique.[10] SiO_2 spheres were prepared using Stober's method.[25] Ruthenium chloride hydrate solution was prepared by dissolving a known amount of 99.98% $RuCl_3{\cdot}xH_2O$ (obtained from Sigma Aldrich) using ethanol as a solvent. Incipient wetness impregnation was carried out in a mortar by dropwise addition of ruthenium chloride solution equivalent to the pore volume of the SiO_2 in a saturated ethanol atmosphere while mixing for 10 min. After impregnation, the sample was dried at 120 °C followed by reduction in 5%H_2/Ar atmosphere at 400 °C for 3 h. Figure 3 shows a typical TEM image of Ru/SiO_2 catalyst after reduction.

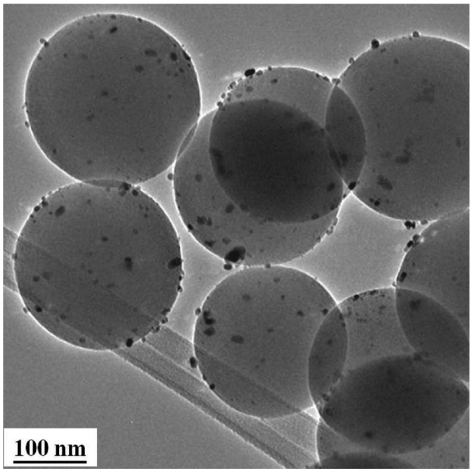

Figure 3. TEM image of 2.5 wt % Ru/SiO_2 catalyst.

TEM sample preparation techniques were developed to create a sample with a sufficiently high catalytic loading for operando TEM. Catalyst was dispersed onto glass wool and was heated to 600 °C in air for about 30 min. At 600 °C, the glass fibers will start to flow and cross-linking takes place between the fibers yielding a material with improved mechanical rigidity. From this mass of wool, a TEM sample was created by cutting a 3 mm diameter disk from the wool. The disk was placed onto an inconel heating holder and was securely sandwiched between inconel washers and a hexring. A small hole was punched in the center of the sample with the help of tweezers. There were many dangling glass fibers protruding from the edge of the hole which were suitable for TEM analysis. Figure 4 shows the low magnification TEM image of Ru/SiO_2 sticking on to the surface of the glass fibers.

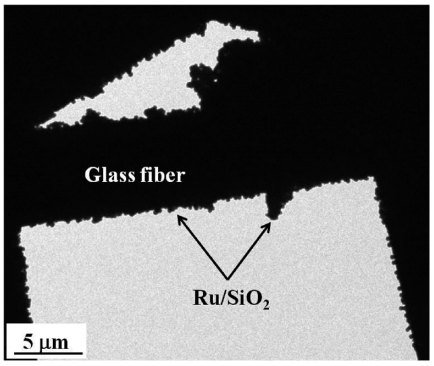

Figure 4. TEM image of glass fiber with Ru/SiO_2 sample loaded.

4. REACTION CONSIDERATIONS FOR OPERANDO TEM EXPERIMENTS

A challenge in performing operando TEM experiment with EELS is related to the differentiation of the gases in the mixture of reactant and product gases in the reaction cell. The reactants and products contain the same elements, and this will lead to

dx.doi.org/10.1021/cs3004853 | ACS Catal. 2012, 2, 2395−2402

significant overlap of the inner-shell ionization edges in the EELS spectrum and it is important to develop methodologies to separate these contributions.

$$CO + \frac{1}{2}O_2 \rightarrow CO_2 \quad (1)$$

CO oxidation is a relatively easy reaction to investigate in terms of differentiating gas phase products from reactants with EELS. Figure 5, panels A and B show the background subtracted inner-shell spectra from pure CO and pure CO_2, respectively, at 1 Torr pressure showing the presence of large π^* peaks in front of the carbon K-edges.[26−28] All the inner shell energy-loss spectra were recorded with the microscope in diffraction mode with an energy dispersion of 0.1 eV.

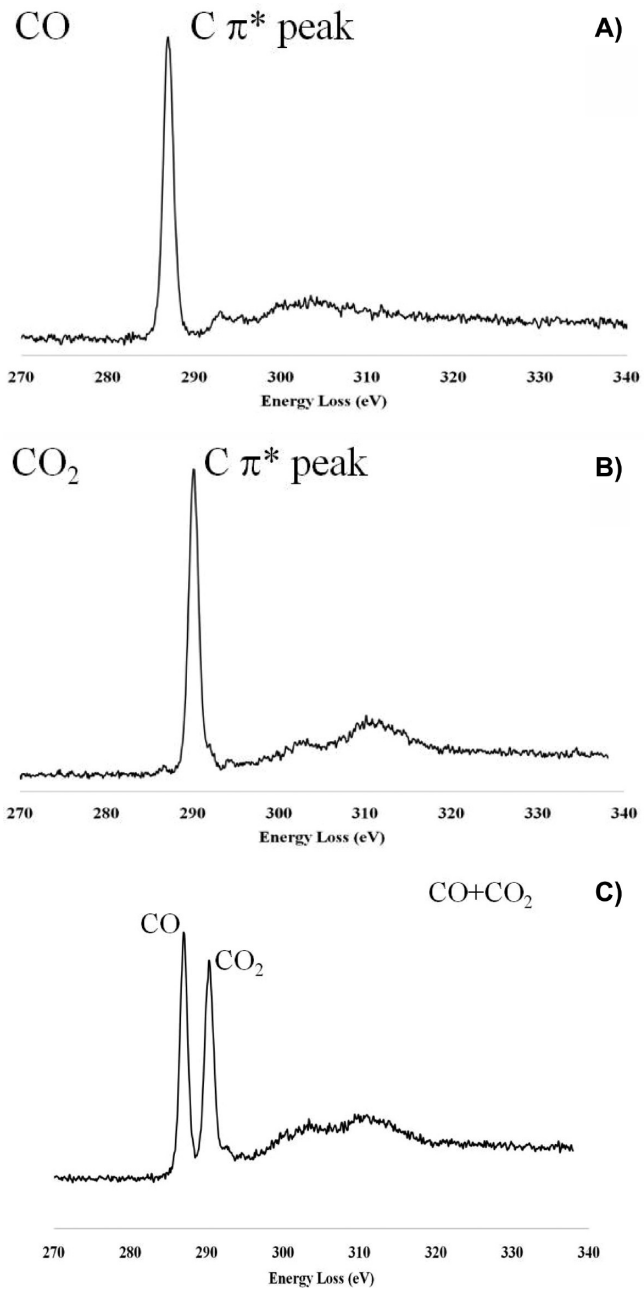

Figure 5. Background subtracted energy-loss spectra from (A) 1 Torr of CO and (B) 1 Torr of CO_2 and (C) normalized EELS spectra from a mixture of CO and CO_2 in 1:1 ratio at 1 Torr pressure.

The π^* peak positions were calibrated with the C K-edge from an amorphous carbon film (284 eV). The C π^* peaks are at 286.4 eV for CO and 289.7 eV for CO_2. The difference of 3.3 eV between the two C π^* peaks is useful for differentiating CO_2 from CO using EELS in an in situ ETEM. Energy-loss spectra were acquired from a mixture of CO and CO_2 in 1:1 ratio, and the background subtracted spectra is shown in Figure 5C. From the figure it is clearly seen that the C π^* peaks of CO and CO_2 are very sharp and easily resolved. During CO oxidation, if significant quantities of CO_2 are produced a peak will be seen at 289.7 eV corresponding to C π^* peak from CO_2.

5. CO OXIDATION ON Ru/SiO_2

The catalytic activity of 2.5 wt % Ru/SiO_2 catalyst for CO oxidation was initially confirmed in the RIG-150 reactor. A 2.5 wt % Ru/SiO_2 catalyst was prepared in the same way as described in section 3, by impregnating SiO_2 spheres with $RuCl_3 \cdot xH_2O$ solution. After impregnation, the sample was dried at 120 °C followed by reduction in $5\%H_2/Ar$ atmosphere at 400 °C for 3 h. Figure 6 shows the performance of the Ru/SiO_2 catalyst for the CO oxidation reaction performed in a RIG-150 reactor. The reaction was performed by flowing $He:CO:O_2$ in 50:8:4 ratio. CO conversion to CO_2 starts at 60 °C; however, the conversions are very low at temperatures below 150 °C. Above 150 °C, CO conversion increases rapidly with increase in temperature with almost all the CO converted to CO_2 by 280 °C.

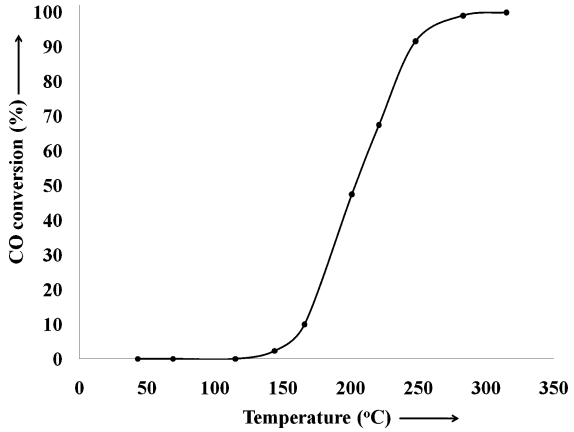

Figure 6. Plot showing the CO conversion during CO oxidation reaction on a Ru/SiO_2 performed in RIG-150 reactor.

In situ catalytic activity measurements were performed in the ETEM on a TEM sample prepared as described in section 3. Ru/SiO_2 was initially reduced in 1 Torr of H_2 at 400 °C for 3 h. After the reduction step, the reactant gas mixture (CO and O_2 in 2:1 ratio) was admitted to the cell, and the pressure was maintained at 1 Torr. Inner-shell energy-loss spectra were collected at different temperatures by slowly ramping up the temperature. Figure 7 shows the background subtracted energy-loss spectra of C π^* peaks obtained while heating the Ru/SiO_2 catalyst inside the environmental cell in the presence of CO and O_2 (2:1) mixture at 1 Torr pressure. A small peak at 289.7 eV was detected at 150 °C corresponding to C π^* peak from CO_2. This observation confirmed that catalysis was taking place inside the TEM. As the temperature was increased, the C π^* peak from CO_2 also increased. To exclude a possible catalytic effect from the inconel furnace of the heating holder, similar

dx.doi.org/10.1021/cs3004853 | ACS Catal. 2012, 2, 2395−2402

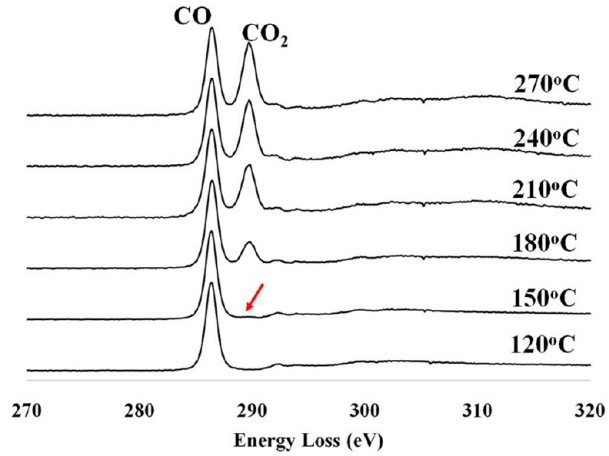

Figure 7. Background subtracted energy-loss spectra acquired at different temperatures during CO oxidation on Ru/SiO_2 catalyst in an ETEM reactor.

experiments were performed with the same holder without the presence of Ru/SiO_2 catalyst. Figure 8 shows the background

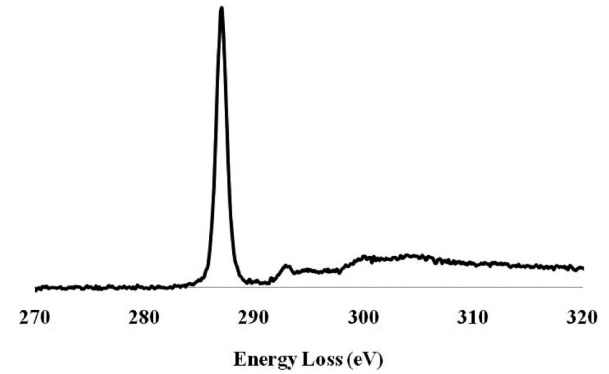

Figure 8. Background subtracted energy-loss spectra acquired at 500 °C during CO oxidation on inconel heating holder.

subtracted energy-loss spectrum of C K-edge from CO and O_2 (2:1) mixture at 500 °C performed on inconel holder. The absence of a C π^* peak at 289.7 eV shows that no detectable CO_2 is present even at 500 °C on the inconel furnace indicating that the product gas measured is due to the catalytic activity of Ru for CO oxidation to CO_2.

This experiment convincingly demonstrates that catalysis was detected in the environmental cell in the TEM and that the Ru catalyst is indeed active. The next step is to quantify the spectroscopic data and determine the catalytic conversion taking place in the environmental cell. Quantification of the catalytic conversion was performed by fitting the energy loss spectra from the gas mixture to a linear combination of individual component reference spectra from CO and CO_2. All the spectra were normalized to unity before performing the fitting. A calibration EELS spectrum was collected from a known mixture of CO and CO_2 to determine the relationship between the linear fitting coefficients and the gas composition. Figure 9 shows the normalized reference spectrum from a mixture of CO and CO_2 in 1:1 ratio (solid curve). The dotted curve shows the fitted composite spectra from the linear combination of CO and CO_2 reference spectra. The spectra from the gas mixture and the composite spectra are almost indistinguishable indicating that a good fit has been achieved.

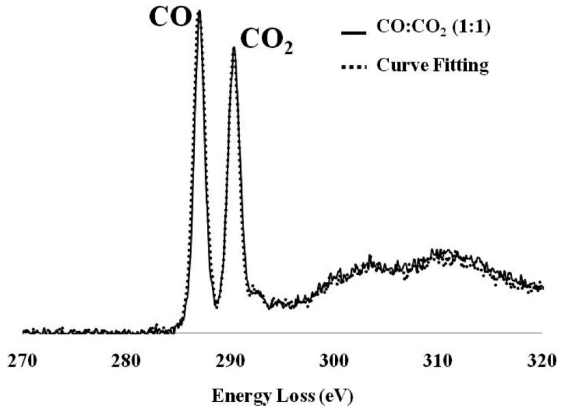

Figure 9. Normalized EELS spectra from a mixture of CO and CO_2 in 1:1 ratio at 1 Torr pressure (solid curve). The dotted curve is the linear combination of the individual spectra from both CO and CO_2.

The ratio of linear coefficients for CO_2 to CO from the curve fitting was obtained to be about 0.95. Since a 1:1 ratio of CO to CO_2 was used, this ratio corresponds to an overall CO conversion in the cell of 50%. Figure 10 shows the

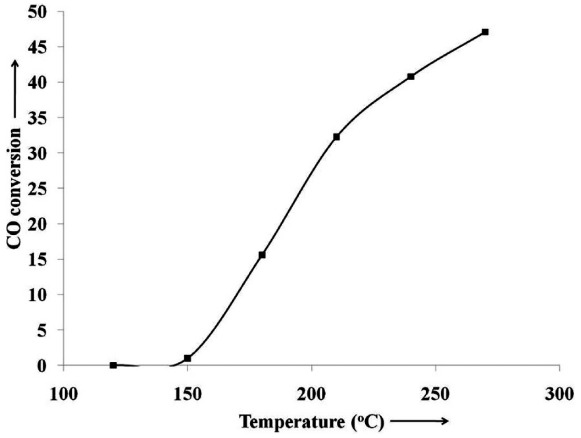

Figure 10. Plot showing the CO conversion with increase in temperature on Ru/SiO_2 catalyst measured from in situ energy-loss spectroscopy.

corresponding CO conversion at different temperatures using a spectral quantification method described above. Catalytic conversion of as low as 1% can be detected with this approach, and the maximum overall conversion in the cell in this case approaches 50% at 270 °C.

6. CO_2 METHANATION ON RU/SIO_2

The example of CO oxidation shows not only that we can detect catalysis in the ETEM but also that the catalytic reaction taking place in the microscope is the same as the reaction taking place in the RIG 150 reactor. This is important because the pressure of the active gas in the ETEM is nearly 50 times smaller than the pressure in the ex situ reactor. However, for pressure sensitive reactions, significant changes in the product distribution may take place between the two reactors. This is demonstrated in our next example where we look at the CO_2 methanation reaction which can be described by the equation

$$CO_2 + 4H_2 \rightarrow CH_4 + 2H_2O \quad (2)$$

dx.doi.org/10.1021/cs3004853 | ACS Catal. 2012, 2, 2395−2402

Figure 11 shows the catalyst performance of 2.5 wt % Ru/SiO_2 for CO_2 methanation (the catalyst was prepared in the same way as that was used for CO oxidation described in section 3) performed in a RIG-150 reactor. CO_2 conversion starts to take place about 290 °C and increases gradually with increase in temperature and reaches 47% at 430 °C. The conversion remains almost constant in the temperature range of 430 to 550 °C. Above 550 °C, the CO_2 conversion increased slowly and reached 75% at 800 °C. CH_4 is the initial product that formed at 290 °C during CO_2 methanation; above 290 °C small quantities of CO form along with the CH_4. Up to 490 °C, the main product gas formed is CH_4 with small quantities of CO. Above 490 °C, CO selectivity increased gradually with a corresponding decrease in the CH_4 selectivity, and almost all the converted CO_2 generates CO at 800 °C.

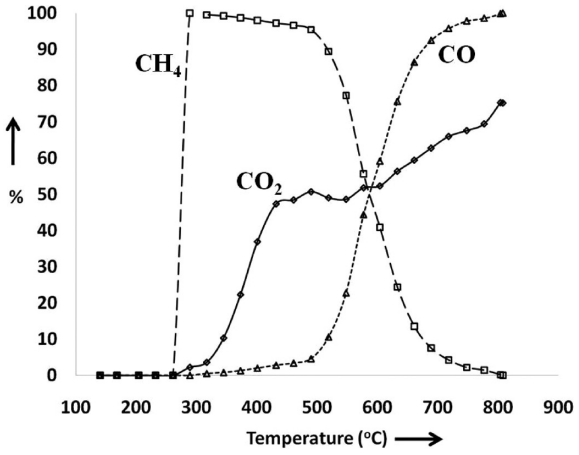

Figure 11. Plot showing the CO_2 conversion and its selectivity to CH_4 and CO with increase in temperature during CO_2 methanation on 2.5 wt % Ru/SiO_2 catalyst in RIG-150 reactor.

In situ catalytic measurements were performed on Ru/SiO_2 catalyst prepared for TEM as described earlier. A CO_2 and H_2 gas mixture was admitted to the environmental cell of the TEM in 1:4 pressure ratio, and EELS spectra were collected at different temperatures. In situ ETEM experiments were performed up to a temperature of 500 °C. Inner-shell energy loss peaks positions of C K-edge from CO_2, CO, and CH_4 are 289.7, 286.4, and 287.9 eV, and this difference in peak position can be used to detect and differentiate between different gas products.

Figure 12 shows the background subtracted C K-edge spectra in the presence of CO_2 and H_2 (in 1:4 ratio) at different temperatures. No change in the spectra was observed below 400 °C. A shoulder peak started to appear at 400 °C at about 286.4 eV corresponding to the CO formation, shown in Figure 12A. The shoulder peak increased with increasing temperature as shown in Figure 12B and 12C. It was surprising to see the formation of CO instead of CH_4 which was the main product gas that formed at this temperature from the ex situ reactor data. The difference between the reactor experiments and the in situ experiments was the gas pressure in the two reactors. In the RIG 150 reactor, experiments were performed at 1 atm by flowing He:CO_2:H_2 in 50:4:16 (partial pressure of CO_2 and H_2 in the gas feed 43 and 172 Torr respectively). In the ETEM reactor, experiments were performed at 1 Torr of gas pressure with partial pressure of CO_2 and H_2 at 0.2 and 0.8 Torr, respectively. This pressure difference changes the product gas distribution resulting in this case. Figure 13 shows the TEM image of Ru/SiO_2 catalyst in the presence of CO_2 and H_2 in 1:4 ratio at 500 °C taken in parallel while measuring the catalytic performance. High resolution microscopy studies were difficult to perform on this sample because of the instabilities caused by the dangling fibers. Further studies are required for simultaneous determination of surface structure of the sample while measuring the catalytic performance. Quantification of CO_2 conversion to CO during the catalysis can be obtained using procedures similar to those used for the CO oxidation reaction in section 5. Figure 14 shows the plot of CO_2 conversion to CO in the presence of 1 Torr of CO_2 and H_2 mixture (in 1:4 ratio) at different temperatures performed in an in situ ETEM.

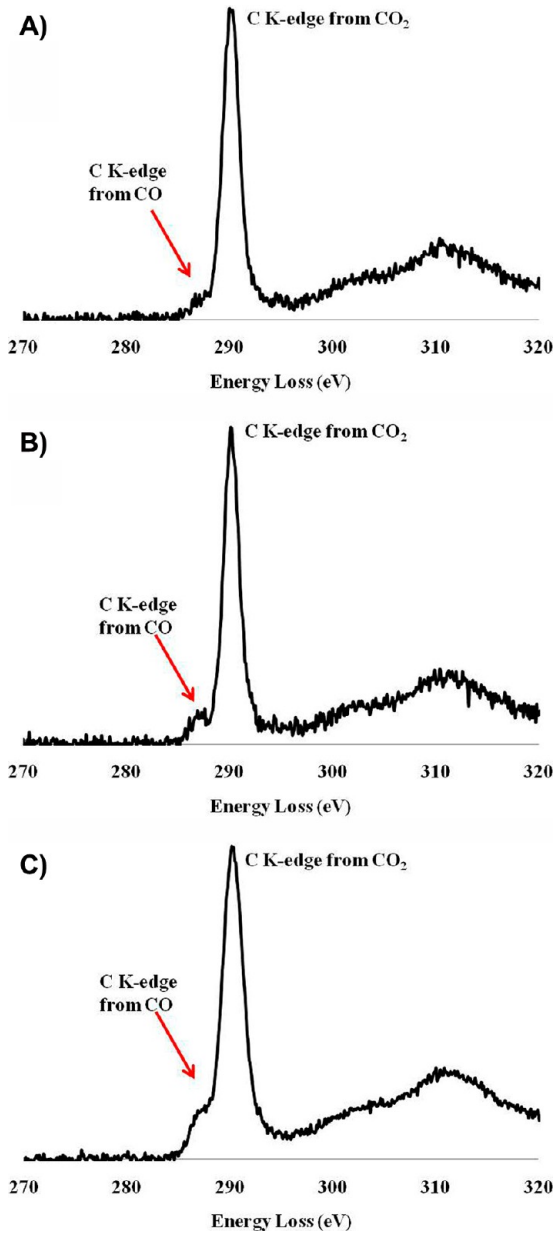

Figure 12. Background subtracted energy-loss spectra of C K-edge acquired at different temperatures during CO_2 methanation on Ru/SiO_2 catalyst in an ETEM reactor at (A) 400 °C, (B) 450 °C, and (C) 500 °C.

dx.doi.org/10.1021/cs3004853 | ACS Catal. 2012, 2, 2395−2402

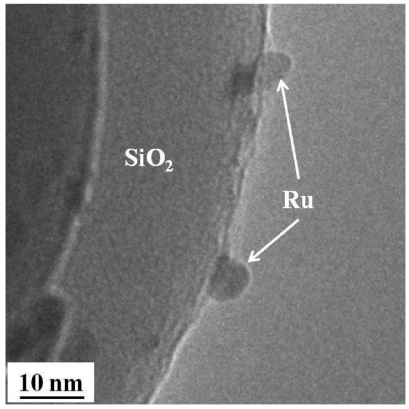

Figure 13. TEM image of Ru/SiO_2 during CO_2 methanation in an in situ ETEM.

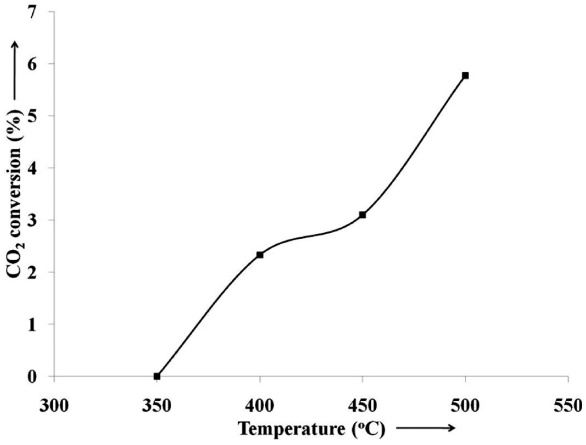

Figure 14. Plot showing the amount of CO_2 conversion to CO with increase in temperature during CO_2 methanation on Ru/SiO_2 catalyst measured from in situ energy-loss spectroscopy.

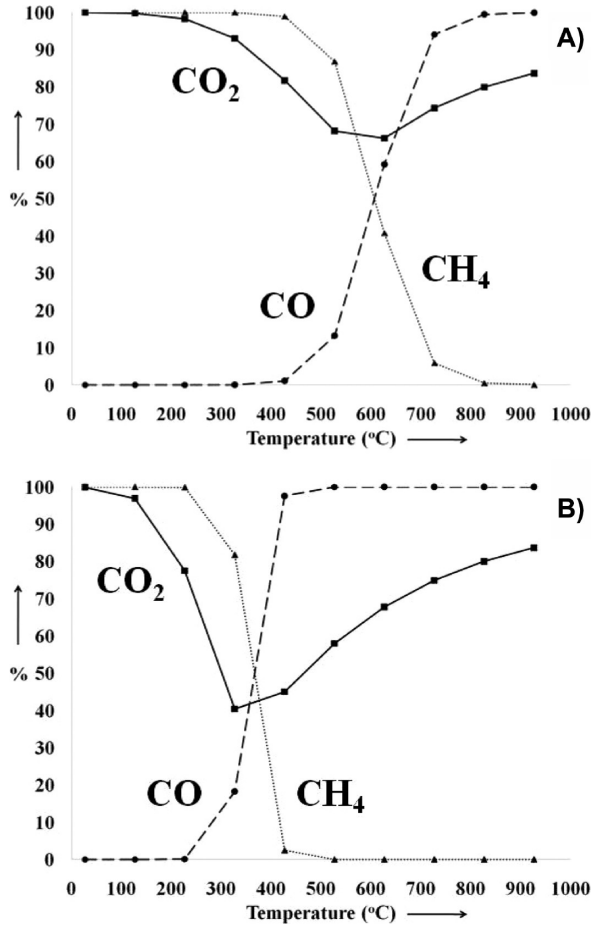

Figure 15. Plot showing the thermodynamic equilibrium calculations of CO_2 conversion to CH_4 and CO at (A) 1 atm and (B) 1 Torr.

To check the effect of pressure, thermodynamic calculations were performed for this reaction using the FACTSAGE program.[29] Figure 15A and 15B shows the plots for CO_2 conversion to CH_4 and CO obtained from the FACTSAGE program for CO_2 methanation reaction at 1 atm and 1 Torr, respectively. From this thermodynamic data, the main product gas in the temperature range of 400 to 500 °C at 1 atm is CH_4 which is similar to the reactor data and at 1 Torr it is CO which is consistent with the in situ ETEM data. These experimental observations demonstrate the importance of operando TEM studies. To develop direct structure−reactivity relationships, structural characterization of the catalyst must be performed while simultaneously measuring the catalytic performance.

CONCLUSIONS

Electron energy-loss spectroscopy was successfully used to directly detect and quantify catalysis taking place inside an environmental cell of the TEM. Proof of concept reactions on CO oxidation and CO_2 methanation were performed to demonstrate the feasibility of an "Operando TEM" methodology for simultaneous measurement of the catalyst activity and nanostructure. One of the challenges in developing an operando TEM technique is to prepare a TEM sample with a large amount of catalyst, so that sufficiently high catalytic conversions can take place giving product gases that can be detectable by EELS. A new sample preparation technique was successfully developed and adopted for performing operando studies.

For CO oxidation, catalytic conversion of as low as 1% can be detected with this approach and the maximum overall conversion in the cell in this case approaches 50% at 270 °C. For the CO_2 methanation reaction, a difference in the product gas formation was observed in the ETEM reactor compared to the quartz tube reactor. This difference in the product gas formation is attributed to the pressure gap that exists between the two reactors. The CO_2 methanation reaction further emphasized the importance of "operando TEM" studies. To develop direct structure−reactivity relationships, structural characterization of the catalyst must be performed while simultaneously measuring the catalytic performance.

This paper demonstrated the first examples in applying EELS in detecting catalysis inside the environmental cell of a microscope. One of the challenges for operando TEM technique is the peak overlap between the reactant and the product gases. Use of monochromated electron microscopes will help to overcome this peak overlap issue and greatly enhance the ability to detect complex product distributions. Moreover, the operando TEM technique will be more powerful in developing the structure−reactivity relationship in heterogeneous catalysis when implemented on a state of the art aberration corrected TEM.

dx.doi.org/10.1021/cs3004853 | ACS Catal. 2012, 2, 2395−2402

AUTHOR INFORMATION

Corresponding Author

*E-mail: crozier@asu.edu. Phone: 480-965-2934. Fax: 480-727-9321.

Notes

The authors declare no competing financial interest.

ACKNOWLEDGMENTS

This work was supported by the NSF CBET 1134464. The use of ETEM at John M. Cowley Center for High Resolution Microscopy at Arizona State University is gratefully acknowledged.

REFERENCES

(1) *Market Report, Global Catalyst Market*, 2nd ed.; Acmite Market Intelligence: Ratingen, Germany, 2011.
(2) Baker, R. T. K.; Chludzinski, J. J. *J. Phys. Chem.* **1986**, *90*, 4734−4738.
(3) Hansen, P. L.; Wagner, J. B.; Helveg, S.; Rostrup-Nielsen, J. R.; Clausen, B. S.; Topsoe, H. *Science* **2002**, *295*, 2053−2055.
(4) Gai, P. L.; Boyes, E. D.; Helveg, S.; Hansen, P. L.; Giorgio, S.; Henry, C. R. *MRS Bull.* **2007**, *32*, 1044−1050.
(5) Gai, P. L. *Top. Catal.* **1999**, *8*, 97−113.
(6) Li, P.; Liu, J.; Nag, N.; Crozier, P. A. *J. Phys. Chem. B* **2005**, *109*, 13883−13890.
(7) Li, P.; Liu, J.; Nag, N.; Crozier, P. A. *Surf. Sci.* **2006**, *600*, 693−702.
(8) Li, P.; Liu, J.; Nag, N.; Crozier, P. A. *Appl. Catal., A* **2006**, *307*, 212−221.
(9) Li, P.; Liu, J.; Nag, N.; Crozier, P. A. *J. Catal.* **2009**, *262*, 73−82.
(10) Banerjee, R.; Crozier, P. A. *J. Phys. Chem. C* **2012**, *116*, 11486−11495.
(11) Wang, R.; Crozier, P. A.; Sharma, R.; Adams, J. B. *Nano Lett.* **2008**, *8* (3), 962−967.
(12) Wang, R.; Crozier, P. A.; Sharma, R. *J. Phys. Chem. C* **2009**, *113*, 5700−5704.
(13) Chenna, S.; Banerjee, R.; Crozier, P. A. *ChemCatChem* **2011**, *3*, 1051−1059.
(14) Chenna, S.; Crozier, P. A. *Micron* **2012**, *43* (11), 1188−1194.
(15) Bañares, M. A.; Wachs, I. E. *J. Raman Spectrosc.* **2002**, *33*, 359−380.
(16) Oleshko, V.; Crozier, P. A.; Cantrell, R.; Westwood, A. *J. Electron Microsc.* **2002**, *51* (Supplement), S27−S39.
(17) Sharma, R.; Iqbal, Z. *Appl. Phys. Lett.* **2004**, *84*, 990−992.
(18) Ross, F. M.; Tersoff, J.; Reuter, M. C. *Phys. Rev. Lett.* **2005**, *95* (146106), 1−4.
(19) Sharma, R.; Moore, E.; Rez, P.; Treacy, M. M. J. *Nano Lett.* **2009**, *9* (2), 689−694.
(20) Crozier, P. A.; Chenna, S. *Ultramicroscopy* **2011**, *111*, 177−185.
(21) Goodman, D. W.; Peden, C. H. F.; Chen, M. S. *Surf. Sci.* **2007**, *601*, L124−L126.
(22) Over, H.; Muhler, M.; Seitsonen, A. P. *Surf. Sci.* **2007**, *601*, 5659−5662.
(23) Sharma, S.; Hu, Z.; Zhang, P.; McFarland, E. W.; Metiu, H. *J. Catal.* **2011**, *278*, 297−309.
(24) Mori, S.; Xu, W. C.; Ishidzuki, T.; Ogasawara, N.; Imai, J.; Kobayashi, K. *Appl. Catal., A* **1996**, *137*, 255−268.
(25) Stober, W.; Fink, A.; Bohn, E. *J. Colloid Interface Sci.* **1968**, *26*, 62−69.
(26) Hitchcock, A. P. *J. Electron Spectrosc. Relat. Phenom.* **2000**, *112* (1−3), 9−29.
(27) Hitchcock, A. P.; Brion, C. E. *J. Electron Spectrosc. Relat. Phenom.* **1980**, *18* (1−2), 1−21.
(28) Hitchcock, A.; Mancini, D. C. *J. Electron Spectrosc. Relat. Phenom.* **1994**, *67* (1), 1−132.
(29) Bale, C. W.; Chartrand, P.; Degterov, S. A.; Eriksson, G.; Hack, K.; Ben Mahfound, R.; Melancon, J.; Pelton, A. D.; Petersen, S. *Calphad* **2002**, *26* (2), 189−228.